Macroroughness and variations in reach-averaged flow resistance in steep mountain streams

M. Nitsche,[1] D. Rickenmann,[1] J. W. Kirchner,[1] J. M. Turowski,[1] and A. Badoux[1]

Received 6 March 2012; revised 20 September 2012; accepted 23 October 2012; published 18 December 2012.

[1] Steep mountain streams typically feature macroroughness elements like large immobile boulders or channel-spanning bedforms such as step-pool sequences. The effects of macroroughness on resistance and flow velocity are not well understood and appropriate field parameters for representing macroroughness in flow velocity equations have not been identified. The prediction of flow velocity in rough and steep streams therefore remains challenging. We measured flow velocity and several macroroughness parameters, i.e., boulder concentration, boulder diameter and protrusion, and roughness of longitudinal channel profiles in six reaches of steep mountain streams with plane bed/riffle, step-pool, and cascade channel morphologies. The between-site variations in flow resistance can be explained to a large degree by nondimensionalization of discharge and flow velocity using channel slope and a characteristic roughness length. Using any of our roughness parameters as the characteristic roughness length, this nondimensionalization leads to a similarity collapse of the entire data set. The remaining differences in flow resistance among the streams are related to dimensionless measures of macroroughness that describe the concentration of boulders or step density in a reach. Boulder concentration represents the measure best describing the data and is used in a simple regression equation for flow velocity. The predictions were better than predictions by the variable power law equation proposed by Ferguson. Although the regression might not be statistically significant, the observed trends suggest that boulder concentration partly explains the residual variance of between-site variation of flow resistance.

Citation: Nitsche, M., D. Rickenmann, J. W. Kirchner, J. M. Turowski, and A. Badoux (2012), Macroroughness and variations in reach-averaged flow resistance in steep mountain streams, *Water Resour. Res.*, *48*, W12518, doi:10.1029/2012WR012091.

1. Introduction

[2] Steep streams (here, streams with gradients greater than about 2%) occupy the majority of the total stream length in mountainous areas. Typically they differ from low-gradient streams by their greater roughness, characterized by wide grain size distributions, variable channel widths, large bedforms, and shallow flows. These streams are important agents of erosion and sediment transfer from headwaters to lower basins. Sediment mobility controls natural channel dynamics, and high-intensity sediment transport episodes pose hazards for buildings, water intakes, and other infrastructure in or near streams. To accurately predict bed load transport rates it is often necessary to estimate the reach-average shear stress, i.e., flow resistance. In steep streams, however, reliable flow resistance estimates require a better understanding of the effects of channel roughness.

[3] Flow velocity is mainly a function of the flow depth h (or the hydraulic radius R_h), the gravitational acceleration g in the direction of the channel slope S, and the channel roughness. The relationship between these parameters is most commonly described with the Darcy-Weisbach equation:

$$v = \frac{\sqrt{8ghS}}{f_{\mathrm{tot}}}, \tag{1}$$

where v is the mean flow velocity and f_{tot} is the dimensionless Darcy-Weisbach friction factor, which scales with a roughness length. The friction factor is an empirical value that is highly variable over time and between individual stream reaches and is difficult to measure in the field. However, it remains crucial for the calculation of flow velocity.

[4] For rough mountain streams it was found that the performance of depth-based flow resistance equations is poor [*Marcus et al.*, 1992]. Alternatively, several authors have proposed nondimensional hydraulic geometry equations that link the mean flow velocity to total water discharge Q [*Rickenmann*, 1994; *Rickenmann*, 1996] or unit discharge q [*Aberle and Smart*, 2003; *Comiti et al.*, 2007; *Ferguson*, 2007; *Rickenmann*, 1994; *Rickenmann*, 1996; *Zimmermann*, 2010], because discharge is much easier to determine in rough streams than flow depth. These equations are given in dimensionless form:

$$v^* = cq^{*m}S^{(1-m)/2}, \tag{2}$$

[1]Mountain Hydrology and Mass Movements, WSL Swiss Federal Institute for Forest, Snow and Landscape Research, Birmensdorf, Switzerland.

Corresponding author: M. Nitsche, Mountain Hydrology and Mass Movements, WSL Swiss Federal Institute for Forest, Snow and Landscape Research, Birmensdorf, Switzerland. (manuel.nitsche@gmail.com)

0043-1397/12/2012WR012091

where $v^* = v/(gD_{84})^{0.5}$, $q^* = q/(gD_{84}{}^3)^{0.5}$, q is the discharge per unit channel width, D_{84} is the 84th percentile of the grain size distribution, and c and m are an empirically determined prefactor and exponent, respectively. *Ferguson* [2007] showed that this type of equation better describes flow velocity measurements in natural streams than other equations. The dimensionless variables were particularly successful in describing at-a-site variations of flow resistance. To better account for the variations between different sites, it was suggested to include the water surface or channel slope as a further factor [*Aberle and Smart*, 2003; *David et al.*, 2010; *Ferguson*, 2007; *Rickenmann and Recking*, 2011; *Zimmermann*, 2010]. As a consequence, *Rickenmann and Recking* [2011] introduced two new dimensionless variables to describe a large data set using an alternative form of equation (2):

$$v^{**} = cq^{**m}, \tag{3}$$

where $v^{**} = v/(gSD_{84})^{0.5}$ and $q^{**} = q/(gSD_{84}{}^3)^{0.5}$. These new variables resulted in a similarity collapse of a large data set in the study by *Rickenmann and Recking* [2011].

[5] Both *Ferguson* [2007] and *Rickenmann and Recking* [2011] used the characteristic grain size D_{84} as the single explicit roughness measure. A characteristic grain size is also used in the standard logarithmic (Keulegan type) or power law equations (Manning-Strickler type). However, in order to allow for form drag on protruding clasts in shallow flows, the characteristic grain size is usually increased by multiplying it by an empirical factor [*Bathurst*, 1985; *Bray*, 1979; *Hey*, 1979; *Thompson and Campbell*, 1979].

[6] *Aberle and Smart* [2003] and *Lee and Ferguson* [2002], among others, have argued that grain size might not be an appropriate roughness measure in steep streams. *Aberle and Smart* [2003] found that hydraulic roughness varied among different sites or different flows even though the characteristic grain size (for example D_{84}) remained the same. Instead, they identified the standard deviation of bed elevation s as a roughness parameter that additionally accounts for the arrangement of grains [*Aberle and Smart*, 2003; *Smart et al.*, 2002].

[7] Steep streams typically feature large grains that can be randomly distributed in the channel, organized in patches or clusters [e.g., *Lamarre and Roy*, 2008; *Nelson et al.*, 2009], or in channel-spanning steps [e.g., *Chin and Wohl*, 2005; *Church and Zimmermann*, 2007; *Whittaker and Jaeggi*, 1982; *Zimmermann et al.*, 2008]. These macroroughness features lead to additional flow resistance that is absent in lower gradient channels. In low-gradient streams the main source of resistance is skin friction, i.e., from drag on individual particles and viscous friction on their surfaces [*Ferguson*, 2007]. In steep streams, by contrast, flow resistance mainly results from macroroughness, including form drag around large boulders due to acceleration, deceleration, and turbulent wakes, as well as spill loss, particularly behind steps or larger particles if flow is locally supercritical [*Chin*, 2003; *Ferguson*, 2007]. *Zimmermann* [2010] concluded that a major part of the flow energy in steep streams is dissipated by form and spill drag around roughness elements like step-pools, as it was also discussed by *Comiti et al.* [2009], *MacFarlane and Wohl* [2003], and *Wilcox et al.* [2006]. The contribution of these structures to total flow resistance increases with increasing relative protrusion (or equivalently, with decreasing relative submergence of the bed).

[8] Macroroughness features are rarely taken into account explicitly in flow resistance equations. The effects of boulder diameter and areal boulder concentration on flow resistance have been studied in laboratory flumes, resulting in empirical or semitheoretical resistance equations [*Pagliara and Chiavaccini*, 2006; *Whittaker et al.*, 1988; *Yager*, 2006; *Yager et al.*, 2007]. Other equations include the effects of steps and pools on flow resistance, using step height and step length as the relevant measures of macroroughness [*Canovaro and Solari*, 2007; *Egashira and Ashida*, 1991; *Whittaker*, 1986]. There are few systematic tests of these approaches using field observations [e.g., *Nitsche et al.*, 2011].

[9] For some mountain streams with very pronounced step-pool structures, *Comiti et al.* [2007] and *David et al.* [2010] found that variations in flow resistance were mostly explained by unit discharge and slope, whereas R_h/D_{84} was not an appropriate explanatory variable. *David et al.* [2010] also found that the relations between flow resistance and these variables were distinct for different channel types. *MacFarlane and Wohl* [2003] found a significant positive correlation between flow resistance and step height-to-length ratio in some step-pool reaches, demonstrating the increasing effect of spill resistance with increasing step height. Detrended standard deviation of bed elevations and relative bed form submergence explained a large portion of the variance in measured flow resistance coefficients and dimensionless velocity in a study of *Yochum et al.* [2012]. Their field data indicate an empirical relation between flow resistance and the relative submergence of bedforms, which supports previously published laboratory findings. Moreover, using detrended standard deviation of elevations instead of D_{84} provided relatively accurate flow velocity predictions for their data set. For some cascade and plane bed channels *Reid and Hickin* [2008] found that among various roughness measures the sorting coefficient D_{84}/D_{50} correlated well with form roughness.

[10] Currently there is no agreement on how best to relate flow resistance to bed properties in steep or shallow streams. This is partly due to (1) a disagreement over how to quantify roughness, and (2) a scarcity of combined flow and roughness measurements in the field. Furthermore, roughness is often described using a single parameter, and none of the roughness measures proposed so far can completely explain the observed variability of flow velocity among different sites.

[11] In the present study we measured flow velocity over a wide range of discharges, in six stream reaches with widely varying channel bed slopes and grain size distributions. In addition, we quantified macroroughness for each of these stream reaches by measuring characteristic grain sizes, boulder concentrations, and the roughness of the longitudinal channel profiles. These data were used (1) to test how macroroughness can be measured, (2) to evaluate the relations among various measures of macroroughness and channel slope, (3) to compare the flow parameters of different rough streams, and (4) to explain the observed between-site variations in flow velocity and macroroughness, using nondimensional variables and regression analysis.

2. Data and Methods

2.1. Field Sites

[12] Data were collected from five mountain streams located in the Swiss Alps and Prealps (Table 1 and Figure 1). For one stream (Riedbach) we studied two different reaches, and for the four other streams one reach was considered for each. The streams cover a wide spectrum of channel characteristics, with morphologies ranging from plane bed to cascade channel types and step-pool types [after *Montgomery and Buffington*, 1997], with channel slopes ranging from 2% to 38% (Table 3). The plane bed streams are alluvial and the cascade and step-pool reaches are often semialluvial with a relatively thin layer of gravel and boulders. The boulders were rather randomly spaced throughout the reaches. In the two cascade reaches, the boulder concentration is 37% and 29%, respectively, resulting in a cascade-like channel morphology. In these streams each boulder is likely to significantly alter the flow at the next downstream boulders. That means that downstream boulders could be in the wake zone of upstream boulders and do not feel the same drag as the upstream boulders. In the step-pool reaches the boulders also formed channel spanning steps. However, pools are only relevant at low flows and spill resistance is not a major source of energy dissipation. Both in our cascade and step-pool reaches the boulders are likely the dominant roughness elements. Three of the stream catchments feature a significant proportion of forest cover (Table 1), however, only small amounts of woody debris are present in the channels. The steps generally contain few woody debris, thus wood is assumed unimportant as a source of roughness. Our study reaches have either near-vertical banks formed by boulders (Erlenbach, Vogelbach, Riedbach steep, Gornera) or somewhat flatter banks formed by smaller grains or bedrock (Riedbach flat, Spöl). Considering the shape of the channel cross sections, flow above bankfull most likely occurred in our study in Riedbach flat and Spöl.

[13] Measurements of mean flow velocity and roughness were carried out in one reach per stream, except in the Riedbach, where two reaches were selected (Table 3). The length of the study reaches ranged from 11 to 28 times the bankfull stream width, and thus were adequate for relating stream morphology and channel processes [*Montgomery and Buffington*, 1997]. The reaches were chosen for their proximity to gauging facilities and their relative morphological homogeneity. The measurements in the Spöl were carried out during an artificial flooding experiment, in which flow stages were held constant for predefined periods. To enlarge the data set of roughness measurements additional roughness data from eight other Swiss mountain streams were used. These streams include the Rappengraben, Sperbelgraben, Melera, Rotenbach, Schwaendlibach, Lonza, Buoholzbach, and Steinibach, which are characterized in the publication by *Nitsche et al.* [2011].

2.2. Flow Measurements

[14] We studied flows covering a range of up to four orders of magnitude and with a dimension of up to 2.7 times bankfull flow (Tables 2 and 1). For flow measurements the tracer dilution method [e.g., *Foster*, 2000; *Kilpatrick and Wilson*, 1989; *Leibundgut et al.*, 2009] was applied using the fluorescent tracer Uranine (color index 45,350), and for some measurements the salt tracer sodium chloride (see Table 2). At low and intermediate flow conditions Uranine concentrations were measured in situ at a rate of 2 s with one flow-through field fluorometer (model GGUN-FL30), developed at the University of Neuchâtel, Switzerland [*Schnegg*, 2003; *Schnegg and Doerflinger*, 1997]. Salt concentrations were obtained from conductivity measurements at a rate of 1 s. In the Erlenbach and the Vogelbach, we also injected and measured tracer automatically at infrequent

Table 1. Reach and Basin Characteristics (Upstream of Study Reach)

	Spöl	Riedbach Flat	Gornera	Erlenbach	Vogelbach	Riedbach Steep
Basin Area (km^2)	295[a]	14	82	0.7	1.6	16
Basin Elevation Range (m)	1674–3302	2035–4327	2005–4634	1110–1655	1055–1540	1810–4327
Mean Upstream Channel Slope	0.01[b]	0.07	0.14	0.18	0.19	0.16
Lithology	Dolomite, Moraine	Moraine, Gneiss	Moraine, Granite, Ophiolite	Flysch	Flysch	Gneiss
Forest/Glacier Extent (%)	30/0[b]	0/60	0/67[c]	39/0	65/0	1/50
Discharge Regime[d]	regulated[e]	a-glaciaire	a-glaciaire	nivo-pluvial prealpine	nivo-pluvial prealpine	a-glaciaire
Mean Annual Precipitation (mm)	800–1200[f]	2000–3000[f]	610[g]	2300	2200	2000–3000[f]
Estimated Bankfull Flow ($m^3\ s^{-1}$)	15[h]	1.5[h]	undefined[i]	1.7[j]	3[j]	undefined[i]
Froude Number at Bankfull Flow	0.53	0.92	–	0.82	0.72	–
Highest Measured Discharge ($m^3\ s^{-1}$)/ Return Period (years)	regulated[e]	no data	70[k]/no data	14.6[l]/50[l]	6.8/50	no data

[a]Data: Swiss Federal Office for the Environment.
[b]Basin up to reservoir.
[c]*Farinotti et al.* [2009].
[d]After *Weingartner and Aschwanden* [1992a].
[e]Discharge managed by a upstream hydropower plant, which provides ecological minimum discharge (0.7–1.4 $m^3\ s^{-1}$) and one or two reservoir releases per year with artificial flows of up to 70 $m^3\ s^{-1}$.
[f]*Weingartner and Aschwanden* [1992b].
[g]At 1638 m, data: MeteoSwiss.
[h]Estimated from width-discharge relation.
[i]Channel sides grade smoothly into banks and hillslopes.
[j]Discharge for return period of 1.5 years calculated from flood statistics.
[k]*Bezinge* [1999].
[l]*Turowski et al.* [2009].

Figure 1. Study reaches at low-flow conditions grouped by channel type. Plane bed/pool riffle: (a) Spöl (channel slope 0.02), (b) Riedbach flat (0.04); step-pool: (c) Erlenbach (0.12), (d) Vogelbach (0.13); and cascade: (e) Gornera (0.11), (f) Riedbach steep (0.38).

high flows with a self-developed system, without the need of on-site personnel. The tracer concentration curves allowed the identification of tracer travel times; we used the harmonic mean tracer travel time to calculate the reach-averaged flow velocity. The harmonic mean has been identified by *Waldon* [2004] as the theoretically correct, unbiased estimate of the mean velocity. *Zimmermann* [2010] has also experimentally shown that the harmonic mean is the most accurate measure for the mean velocity compared to peak or centroid velocities.

Table 2. Methods and Range of Flow Measurements

Study Reach	Velocity	Velocity Error[a] (%)	Discharge	Discharge Error[a] (%)	N[b]	Flow Range ($m^3\ s^{-1}$)
Spöl	From h, with $v = Q/A(h)$	20	Gauge	10	10	2–40
Riedbach (Flat)	Tracer travel time[c]	10	Tracer dilution	10	20	0.3–2
Gornera	Tracer travel time[c]	10	Stream gauge + tracer	10	10	0.2–20
Erlenbach	Tracer travel time[c,d]	11	Stream gauge	10	78	0.0005–2
Vogelbach	Tracer travel time[c,d]	10	Tracer dilution	10	31	0.04–3
Riedbach (Steep)	Tracer travel time[c]	11	Stream gauge	10	27	0.06–4

[a]Average summed squared relative error (estimated for each stream using uncertainty propagation).
[b]N is the number of measurements.
[c]Dye tracer: Uranine.
[d]Salt tracer: sodium chloride.

[15] In all experiments the tracer was instantaneously injected (slug injection) into a preferably well mixed cross section, assuming that lateral mixing is complete after short distances relative to the reach length. The tracer probe was placed relatively close to the sides of the stream, missing the center of the flow. Both incomplete mixing and probe location cause errors in the velocity measurement. We estimate these errors at a constant 5%. Further sources of uncertainty are (1) the determination of injection time, (2) the sampling rate, and (3) the accuracy of flow path measurement. For each stream the combined uncertainty estimate in flow velocity was individually calculated (Table 2).

[16] Flow discharge was independently measured with stream gauges in four study reaches, and for two reaches it was derived from the tracer concentration curves (Table 2). Uncertainty in discharge gauging is approximately 10%. The uncertainty in the present discharge measurements from tracer concentration curves is mainly affected by the accuracy of the injection mass and the calibration solution. Additionally, the relationship between fluorescence and dye concentration (and thus inferred discharge) is affected by photochemical decay under exposure to light [*Leibundgut et al.*, 2009]. Uranine has a half-lifetime of 11 h in daylight [*GSF*, 1978], and thus Uranine degradation can be neglected at the much shorter exposure times (tens of seconds) during our experiments. Potential errors due to the influence of pH value, temperature, and turbidity on the fluorescence intensity were eliminated through fluorometer calibration just before each measurement. Sorption and filtration of the tracer were assumed to be insignificant, because of the short flow paths (<110 m) and short flow times (tens of seconds). The mean error for the discharge measurements was explicitly calculated for each of the streams (Table 2).

2.3. Hydraulic Parameters

[17] A representative channel cross section was interpolated from the vertical mean of multiple measured cross sections (see example in Figure 2). Using this reach-averaged cross section, we solved for hydraulic parameters (i.e., flow depth h and width w, hydraulic radius R_h, cross sectional area A) corresponding to each measured value of discharge and reach-averaged velocity. Because flow width varies with the discharge Q, the unit discharge was determined by $q = Q/w$, where $w = A/h$. The resulting flow parameters are not exact for any particular cross section in the reach, but instead represent an average of the reach. This reach-averaged approach is justified because we know only the reach-averaged flow velocity, rather than the flow velocity at each cross section.

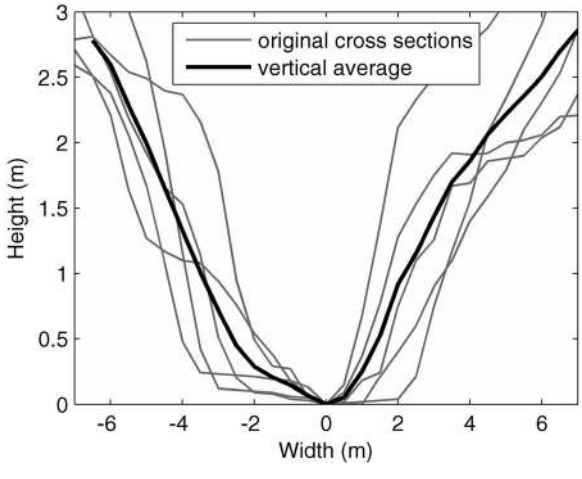

Figure 2. Original cross sections and vertically averaged section of the Erlenbach study reach.

2.4. Macroroughness Measurements

[18] We characterized macroroughness through the grain size distributions and geometric channel parameters of the study reaches. For boulder-based macroroughness measures, we used the mean diameter (D_b) and the concentration (Γ) of large, relatively immobile boulders, where $\Gamma = n_b \pi D_b^2/(4WL_r)$, with n_b the number of boulders, W is the width, and L_r is the length of the reach. Ideally, the definition of a critical boulder diameter should be based on the grain size that is moved at a discharge corresponding to a specific reoccurrence interval or, maybe more importantly, it should be based on flow depth. Since we do not have the necessary information on the frequency of boulder movement and the effect of boulders at different flows, we fixed the critical boulder diameter at 0.5 m and every grain whose b axis was larger than the critical diameter was measured. Our approach might not be valid for shallow flows, for which smaller grains could also represent macroroughness elements. However, the approach allows a more robust data acquisition in the field, where measuring smaller grains would involve greater uncertainties and much greater effort. If the b axis was not identifiable, the longest axis protruding above the channel bed was measured instead.

[19] Longitudinal profiles of the reaches were obtained with a total station or a laser slope and distance meter. Instead of using a fixed point density, the measurements were taken at breaks in slope, as recommended by *Zimmermann et al.* [2008]. The resulting profiles feature a variable horizontal resolution of 0.2–2 m and they were used to identify steps and pools using the step-pool classification approach of *Zimmermann et al.* [2008]. The *Zimmermann et al.* [2008] algorithm is scale-free and independent of the point density of the profiles, and allows derivation of the step height H_s, which is defined here as the vertical distance from the top of a step to the downstream end of its associated pool, and step length L_s, which is the horizontal distance between a step and the next step downstream. From these main step characteristics further parameters were derived, including the step slope H_s/L_s and the step density n/L_r (where n is the number of steps in a reach and L_r is the effective reach length).

[20] The standard deviations of elevations of the longitudinal profiles s were derived by a procedure similar to that of *Smart et al.* [2004]. First, the longitudinal profiles were interpolated to an equidistant point spacing of 0.5 m, in order to have an equal spacing for all streams. Because trends in the elevation data, introduced by channel slope or large bedforms, would blur the scaling region of macroroughness, the profiles were then flexibly detrended. To do this, we inserted knot points into the longitudinal profile at a spacing of 10 times the mean boulder diameter D_b. The elevations at these knot points were determined by averaging all elevations in the original profile within a distance of 5

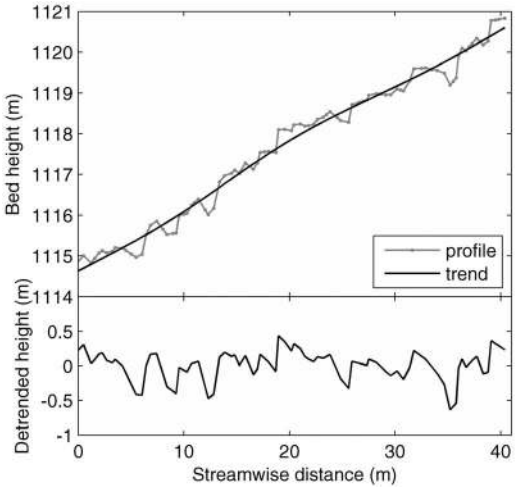

Figure 3. Longitudinal profile of the Erlenbach study reach with trend spline and the resulting detrended profile.

D_b upstream and downstream of each knot point. Cubic spline interpolation was used to interpolate between these knot points to generate a trend line. This trend was then subtracted from the original profile elevations, which removed the slope of any forms larger than the biggest boulders or boulder clusters (Figure 3).

[21] Channel geometry and the measured roughness parameters may vary considerably within a given reach. Therefore, reach-averaged values of roughness and channel geometry were used throughout our analysis. This simplification is adequate, because the analysis is made at the reach scale and, moreover, our flow measurements also represent an average of the flow conditions within the reach (see Table 3 for an overview of the measured parameters and additional definitions).

3. Results

3.1. Relationships Between Roughness Parameters and Slope

[22] In many studies measures of boulders and steps were primarily developed from laboratory experiments to quantify ideal type elements of large-scale roughness. In nature, however, macroroughness elements are generally not distinct or well-defined features. Channel-spanning steps, for example, often co-occur with randomly arranged boulders. The comparison of roughness measures of the 6 + 8 study reaches (Figure 4) identifies various proxy variables and their dependence on slope.

[23] Despite the large range of channel types, the channel slope correlates well with several macroroughness measures, for example with boulder concentration Γ, with the standard deviation of elevation s, and with the boulder protrusion P. This indicates that the effects of channel slope and the effects of roughness cannot be separated in field data from steep streams. Slope S and step features like step slope H_s/L_s and step density n/L_r correlate less significantly in the study reaches. The surprisingly low correlation between D_{84} and the slope S of the study streams is partly due to one outlier. Without this outlier r^2 is 0.66; a correlation between D_{84} and S in rivers is generally expected, although with much scatter around it [*Montgomery and Buffington*, 1997].

[24] There are variable correlations between macroroughness measures. The boulder concentration Γ is significantly correlated with D_{84} (Figure 4); thus, Γ and D_{84} can be considered proxies for each other. The standard deviation of elevations s shows a weak correlation with the step height H_s and D_{84}. There are also pairs of roughness measures that appear independent, for example D_{84} and step height H_s, and boulder concentration Γ and step slope H_s/L_s (Figure 4).

3.2. Variations of Flow Properties With Discharge

[25] Every stream reach shows a well-defined increase in flow velocity v with discharge Q or discharge per unit width q

Table 3. Reach Geometry and Roughness Measures of the Study Reaches

Parameter	Symbol	Spöl	Riedbach Flat	Gornera	Erlenbach	Vogelbach	Riedbach Steep
Channel Type[a]		Pool riffle	Plane bed	Cascade	Step pool	Step pool	Cascade
Channel Slope	S	0.02	0.04	0.11	0.12	0.13	0.38
D_{84}[b] (m)	D_{84}	0.11	0.22	1.17	0.29	0.35	0.86
Bankfull Width[c] (m)	W_{bf}	18.7	6.5	10.7	4.7	5.7	13.0
Bottom Width[c] (m)	W	16.0	6.0	9.0	3.5	5.0	6.0
Mean Boulder Size (m)	D_b	0.70	0.83	0.78	0.82	0.62	0.82
Boulder Protrusion[d] (m)	P	0.41	0.45	0.45	0.51	0.25	0.22
Boulder Concentration[e]	Γ	0.05	0.01	0.29	0.11	0.12	0.37
Boulder Step Spacing[f]	λ_x	14.9	69.7	2.7	7.5	5.3	2.2
Mean Step Height (m)	H_s	–	0.4	0.9	0.4	0.5	1.3
Mean Step Length (m)	L_s	–	7.5	13.1	4.1	5.0	29.1
Step Slope	H_s/L_s	–	0.05	0.07	0.10	0.10	0.05
Reach Length (m)	L_r	53.4	108.4	252.2	40.8	81.6	100.5
Reach Height Difference (m)	H_r	0.9	4.1	28.8	6.0	9.8	34.1
Number of Steps	n	0	3	19	9	12	3
Step Density	n/L_r	0	0.03	0.17	0.22	0.15	0.03
Standard Dev. of Elevations (m)	s	0.07	0.10	0.32	0.26	0.25	0.47

[a]After *Montgomery and Buffington* [1997].
[b]Grain sizes were calculated after *Fehr* [1987] based on line-by-number pebble counts of around 500 grains of down to 1 cm in diameter for each study reach.
[c]Average of field measurements which were taken at least every 10 m.
[d]Upstream height of an boulder that protrudes above the finer bed material, after *Yager et al.* [2007].
[e]Area fraction covered by boulders, after *Pagliara and Chiavaccini* [2006].
[f]After *Yager* [2006].

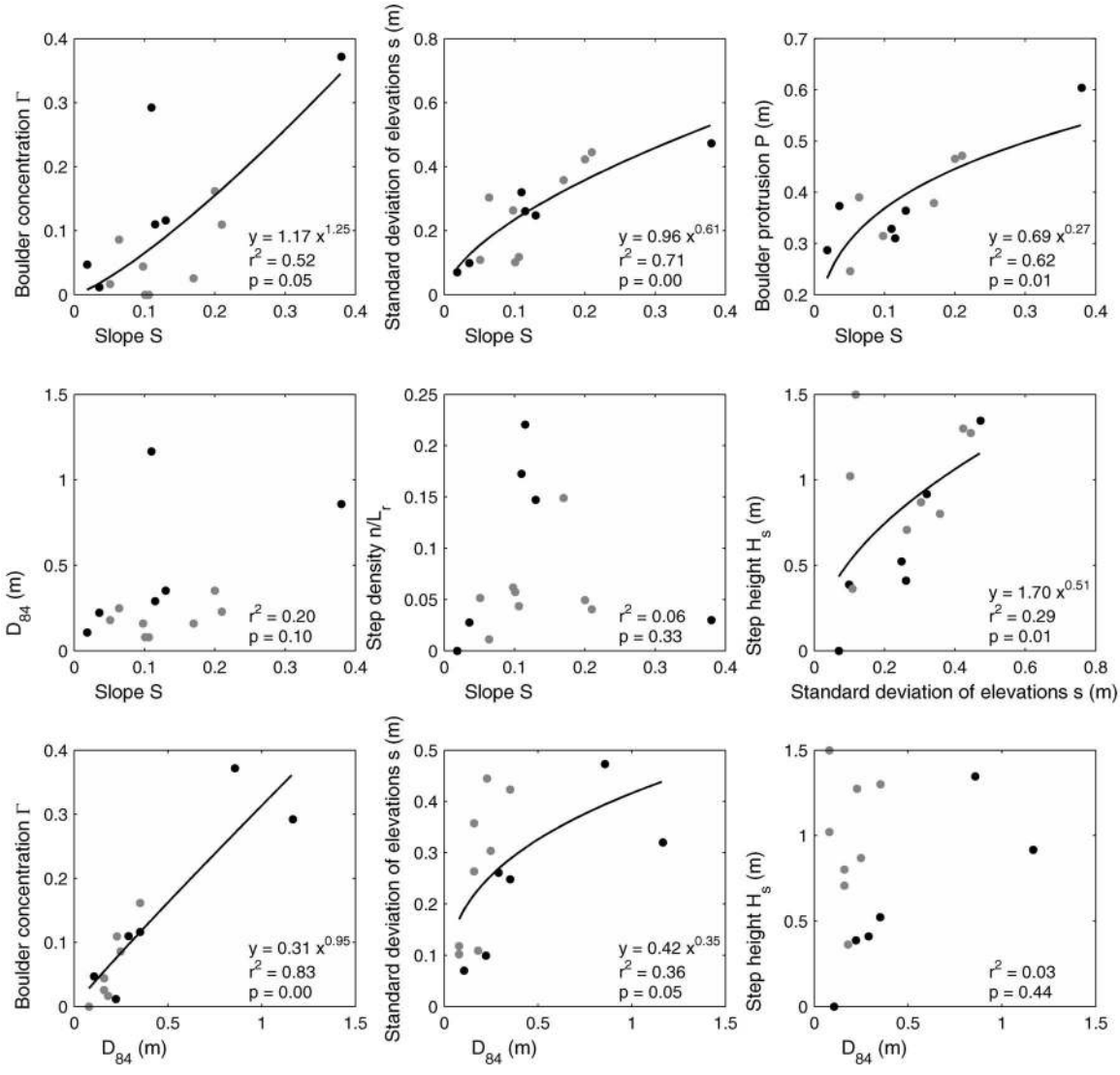

Figure 4. Correlation of roughness measures and channel slope or D_{84} in the six study reaches (black points) and eight additional reaches (gray points, cf. section 2.1). Power law fit lines for the complete data set were drawn when significance level $p \leq 0.05$.

(Figures 5a and 5b). Fitting trends by ordinary least squares, the mean flow velocity scales on average with an exponent of about 0.47 with discharge (Figure 5a), and with an exponent of about 0.6 with unit discharge (Figure 5b). The well defined *v*-*Q* trends have exponents from 0.39 to 0.52. The *v*-*Q* data for each site give a relatively smooth trend with no sharp discontinuities between low and high flows. At higher flows the curves slightly flatten. The different intercepts of the trend lines of the *v*-*Q* relation (Figure 5a) were correlated with measured roughness properties of the channels and no strong relation was found.

[26] Flow resistance was calculated with equation (1) and is plotted against unit discharge q in Figure 5c. The exponents are more variable than in the discharge-velocity plots of Figures 5a and 5b. One reach, Riedbach flat, stands out with a fast decrease in roughness with increasing discharge (exponent 0.66). The exponents for the other five reaches range from 0.31 to 0.47. If the prefactors derived from the trend lines in Figure 5c are compared to the measured roughness properties of the channels, a distinct sorting can be observed. Small prefactors are related to steeper streams, higher boulder concentrations, and a larger standard deviation of elevations. These observations are explained in more detail in the next section.

[27] When flow resistance is plotted against the relative submergence R_h/D_{84}, the data points show some flattening at higher relative submergence (Figure 5d). This flattening is particularly pronounced for Erlenbach, Gornera, Spöl, and Riedbach steep. In these reaches the relation could also be described by two power functions or a variable power law equation instead of one power law. For five reaches, the hydraulic radius R_h is also systematically lower than D_{84}, except at high flows, when they are approximately of the same scale (Figure 5d). These flows would presumably not submerge the roughness elements. One other stream (Spöl) has R_h values that are systematically higher than D_{84}.

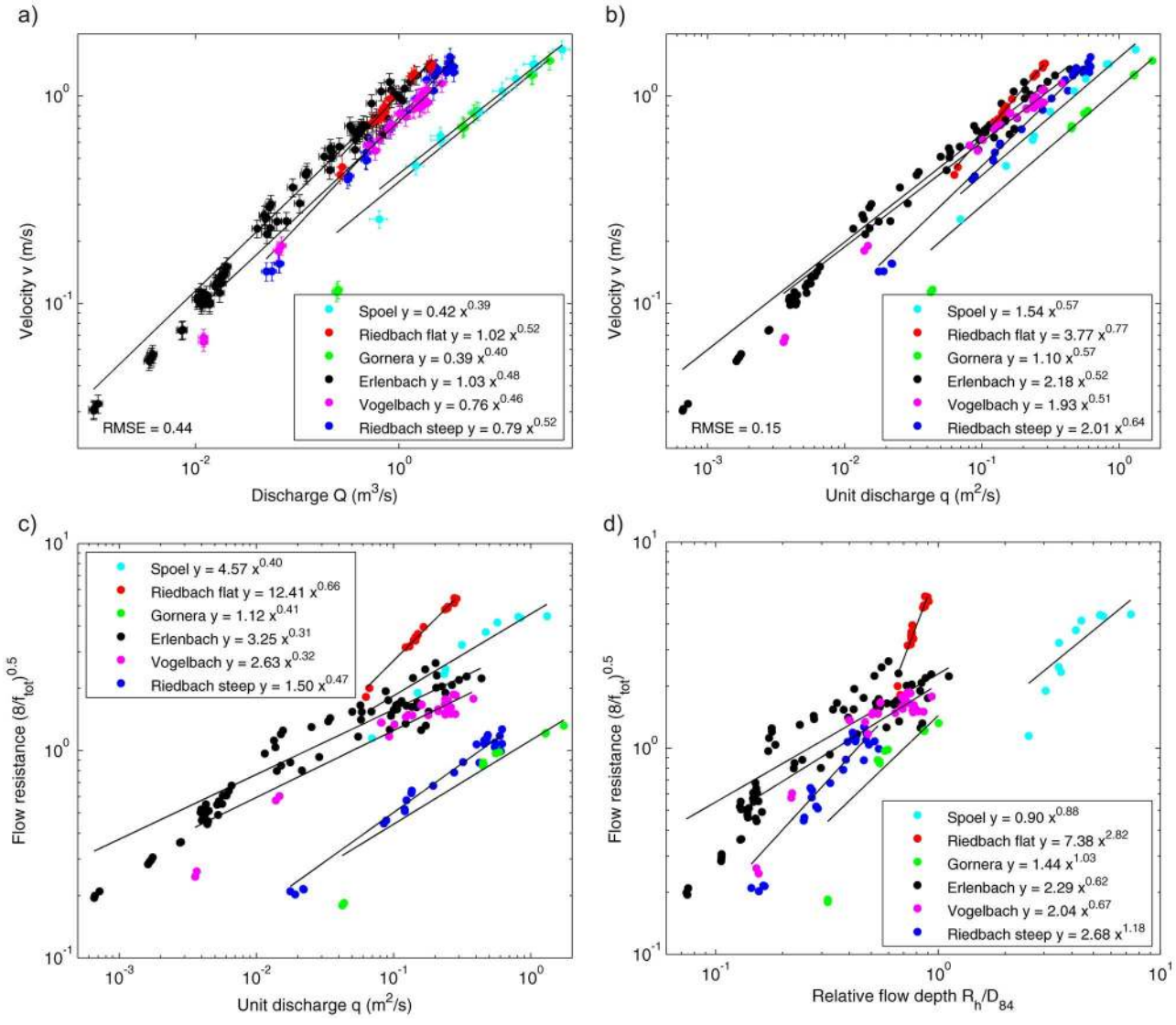

Figure 5. Variation of flow parameters with increasing discharge or relative flow depth. Power law trend lines are fitted to data of each reach. RMSE is the root mean square error of all data in (a) and (b), respectively.

There, high flows could potentially submerge the roughness elements and therefore a faster increase in R_h or h might be expected, compared to the other streams.

3.3. Nondimensionalization of Velocity and Discharge

[28] To better describe the relation between discharge and flow velocity and to obtain a predictive velocity equation, we conducted a dimensional analysis, assuming that the velocity v [L/T] is a function of slope S [L/L], unit discharge q [L^2/T], gravitational force g [L/T^2], and channel roughness R [L]. Viscosity is neglected because we assume fully turbulent flow. The water density ρ drops out, and there is no dimension of mass anywhere else. We assume that S is only relevant as a component of downslope gravitational force, therefore we only work with gS as a combined variable. Note that S and R vary among sites but are constant at each site. Only q varies within each site. With four variables (gS, q, v, R) and two dimensions (T, L), we expect two independent dimensionless groups. There is only one possible pair of nondimensional groups that keeps v and q separate:

$$q^{**} = \frac{q}{\sqrt{gSR^3}}, \tag{4}$$

$$v^{**} = \frac{v}{\sqrt{gSR}}. \tag{5}$$

[29] These nondimensional variables are similar to those introduced by *Rickenmann and Recking* [2011], who used D_{84} as their roughness parameter (R), and thus the analysis above provides a dimensional justification of their variables. As a characteristic channel roughness length we can additionally use our macroroughness measurements, including average step height H_s, standard deviation of elevations s and boulder protrusion P.

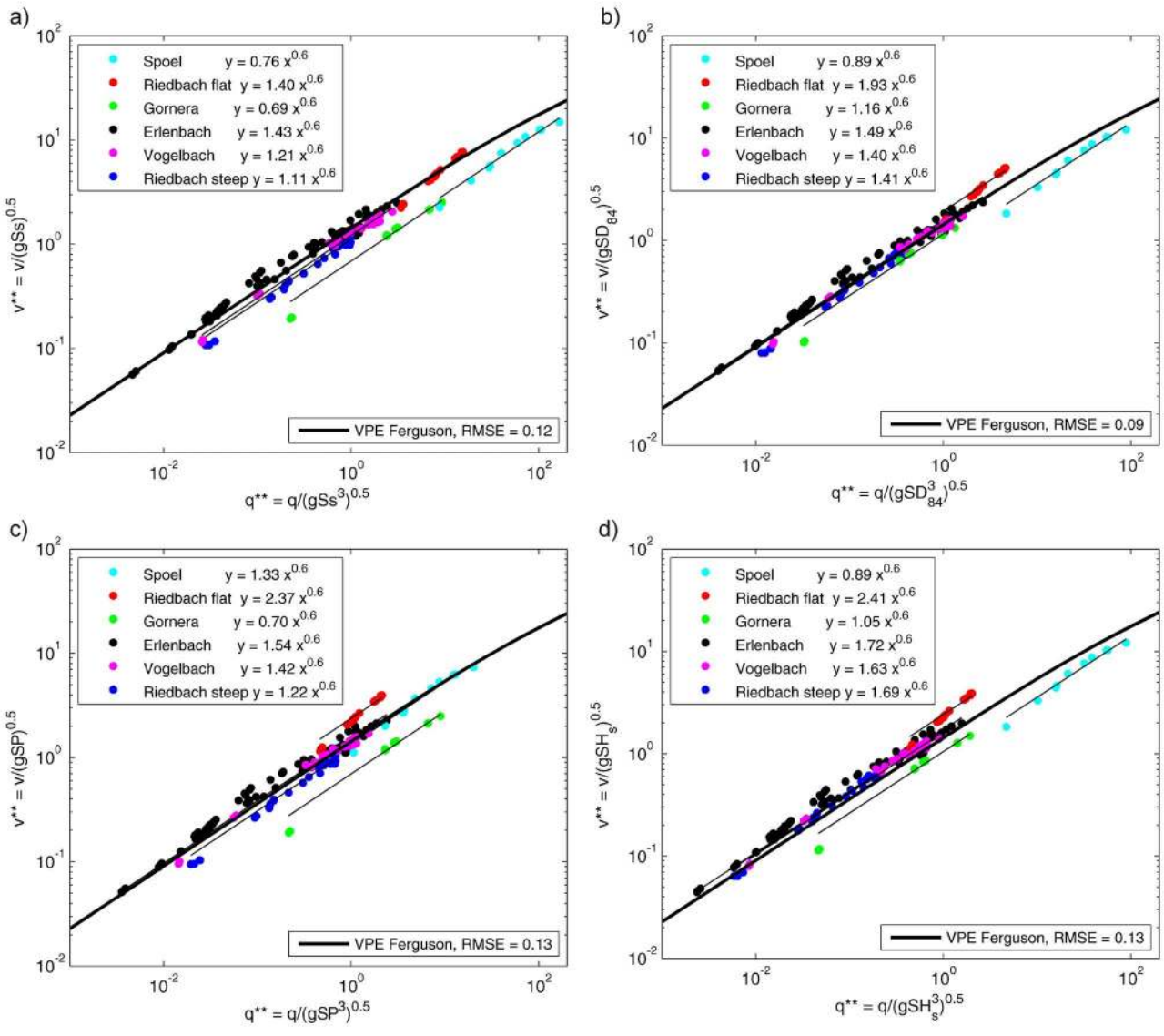

Figure 6. Dimensionless discharge q^{**} against dimensionless velocity v^{**} using different roughness length R: standard deviation of (a) elevations s, (b) grain size D_{84}, (c) boulder protrusion P, and (d) step height H_s. The root mean square error (RMSE) in log units is given for the deviation of all reach data points from the empirically derived VPE (equation (6)) (bold line). Fit equations (with a fixed exponent of 0.6) and fit lines (thin lines) are given for each reach.

[30] The nondimensionalization given by equations (4) and (5) yields a similarity collapse, in which the data from different sites plot close to a single power law relationship, in which v^{**} is almost proportional to the square root of q^{**} (Figure 6). Note that the similarity collapse works almost equally well with the different roughness lengths. As a measure for the form of the collapse we indicated the root mean square error (RMSE) of the data in relation to the variable power law equation (VPE) of *Ferguson* [2007], shown by the thick line in Figure 6. Here, instead of the original form based on flow depth, we used the equivalent q-based form of the VPE as given by *Rickenmann and Recking* [2011], which is equivalent to

$$v^{**} = 1.443 q^{**0.60} \left[1 + \left(\frac{q^{**}}{43.78} \right)^{0.8214} \right]^{-0.2435}. \quad (6)$$

[31] For the measured flow range, the VPE has a slope of 0.6. The tightest similarity collapse of our data was obtained using D_{84} as the roughness measure (RMSE = 0.09), followed by standard deviation of elevations s (RMSE = 0.12), and boulder protrusion P and step height H_s (RMSE = 0.13) (Figure 6).

3.4. Dependence of v^{**} on q^{**} and Dimensionless Roughness

[32] The nondimensional variables v^{**} and q^{**} explain a large portion of the variation in the relation between velocity and discharge. However, the introduced roughness length R did not produce a perfect similarity collapse; there is still variation between the individual sites. While there was no simple relationship between channel macroroughness and the elevations of the trend lines in the v-Q plot (Figure 5a),

there is a systematic relationship between roughness and the trend lines that relate the nondimensional velocity v^{**} and discharge q^{**}. Here we introduce the boulder concentration Γ, the step density n/L_r, and the step slope H_s/L_s as nondimensional roughness parameters R^*, which—in contrast to the dimensional roughness length R—also contain information about the concentration or the character of the roughness elements in the channel. As a rough empirical approximation, we estimated the dependence of v^{**} on q^{**} and R^* by a simple regression analysis. At first, a power law equation was fitted to each data set in the v^{**}-q^{**} relations with the form

$$v^{**} = kq^{**0.6}, \tag{7}$$

where k is the site specific prefactor of the power law fit. The exponent was fixed at 0.6, which approximates the mean of the slopes in Figure 6 and equals the slope of the VPE function for the observed q^{**} range. Then the site-specific prefactors k of equation (7) were related to the nondimensional measures of macroroughness R^*. Linear regression of R^* and the prefactors k give a regression equation with the form

$$k' = a \cdot R^* + b, \tag{8}$$

where k' is the predicted prefactor k of equation (7), and a and b are the empirically derived regression coefficients. Because q^{**} and v^{**} were calculated with four different roughness length, namely D_{84}, s, P, and H_s (see section 3.3), there are also four different relationships between k and the dimensionless roughness measures R^*. As an example, the relationship derived from v^{**} and q^{**} using D_{84} is shown in Figure 7. The relations obtained from the other parameter combinations are given in Table 4. Among the dimensionless roughness parameters, only the boulder concentration Γ has a strong correlation with the prefactor k, regardless of the roughness length R used in the q^{**}-v^{**} relations (Figure 6). The regression coefficients a and b and the correlation coefficient r are given in Table 4. The regression was performed only on five study reaches, excluding the Spöl, because the Spöl exerted substantial overbank flow, resulting in a comparatively higher roughness (because of small R_h/D_{84} values in overbank flow region).

[33] The regression equation (8) for estimating the prefactor k' can be used as input to a predictive equation for flow velocity, here given in dimensional form

$$v_{\text{pred}} = k' q^{**0.6} \sqrt{gSR}. \tag{9}$$

[34] The predictions of equation (9) were compared to the measured absolute velocities, and their agreement illustrates the goodness of the regression. The best predictions were obtained using the v^{**}-q^{**} relation based on $R = D_{84}$ combined with the regression equation for k' using boulder concentration Γ resulting in

$$v_{\text{pred}} = (-1.4\Gamma + 1.73) q^{**0.6} \sqrt{gSD}_{84}. \tag{10}$$

[35] For the predictions of equation (10) and observed flow velocities, the coefficient of determination r^2 is 0.94 (Figure 8). For comparison the flow velocity predictions are also given for the VPE by *Ferguson* [2007], an equation which performed best in the comprehensive test of flow velocity equations by *Rickenmann and Recking* [2011]. The r^2 value of the VPE approach (0.92) was slightly lower than the r^2 obtained with equation (10) (Figure 8). The predictive capabilities of equation (10) and the VPE are also shown using scores of predicted versus observed flow velocity (Table 5). On average with equal weight for all stream reaches our approach predicted 88% of the flow velocity data with a precision of ±20%, whereas the VPE approach achieved a score of 62%.

4. Discussion

4.1. Performance of Nondimensional Variables

[36] Our data set includes flow measurements taken at six reaches at discharges varying by nearly four orders of magnitude. The data thus represent variations in flow resistance both at a site and between sites. The dimensionless variables $v^* = v/(gD_{84})^{0.5}$ and $q^* = q/(gD_{84}{}^3)^{0.5}$ as used in equation (2) have been successfully used to describe at-a-site variations of flow resistance in various studies [*Rickenmann and Recking*, 2011]. To explain variations between different sites it has been found to be important to account for the

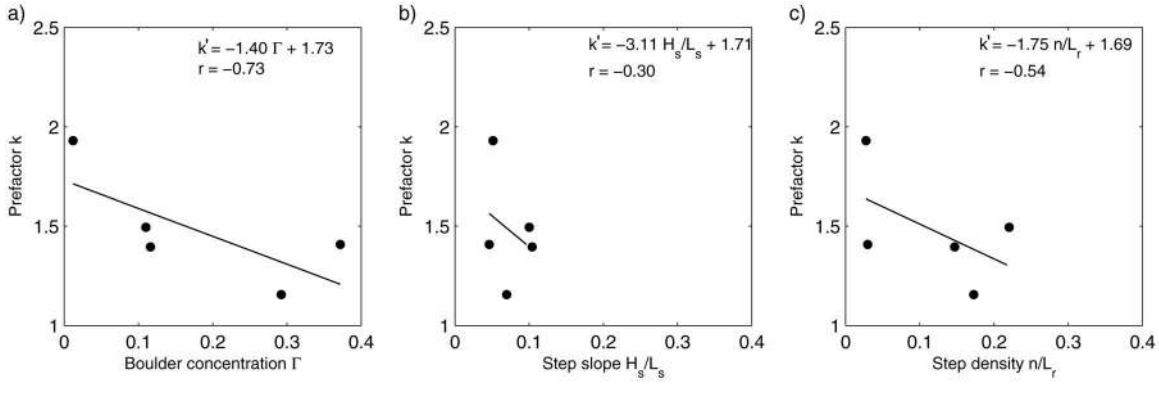

Figure 7. The prefactor k as a function of dimensionless roughness measures. Lines are fitted linear trends given by $k' = aR^* + b$ (equation (8)). The prefactor k was derived from the v^{**}-q^{**} relation using $R = D_{84}$.

Table 4. Correlation of Dimensionless Macroroughness R^* With Prefactor k[a]

	k From q^{**}-v^{**} ($R = D_{84}$)			k From q^{**}-v^{**} ($R = P$)			k From q^{**}-v^{**} ($R = s$)			k From q^{**}-v^{**} ($R = H_s$)		
R^*	r	a	b	r	a	b	r	a	b	r	a	b
Γ	−0.73	−1.40	1.73	−0.80	−3.31	2.05	−0.71	−1.44	1.43	−0.68	−2.22	2.10
H_s/L_s	−0.30	−3.11	1.71	−0.16	−3.57	1.71	0.21	2.34	0.99	−0.28	−5.02	2.07
n/L_r	−0.54	−1.75	1.69	−0.46	−3.20	1.83	−0.13	−0.44	1.22	−0.59	−3.26	2.09

[a]The prefactor k was derived from the q^{**}-v^{**} relation, using various roughness length R. r is the coefficient of correlation, a and b are the regression coefficients in the regression equation $k' = aR^* + b$ (equation (8)).

channel slope as a further factor [*Aberle and Smart*, 2003; *David et al.*, 2010; *Ferguson*, 2007; *Rickenmann*, 1994; *Rickenmann and Recking*, 2011; *Zimmermann*, 2010]. In the present study we used two slightly modified dimensionless variables that include the factor slope: $v^{**} = v/(gSD_{84})^{0.5}$ and $q^{**} = q/(gSD_{84}{}^3)^{0.5}$ (as used in equation (3)). These variables were previously introduced by *Rickenmann and Recking* [2011] to better investigate the transitional behavior between shallow and deep flows and they achieved a similarity collapse for a large data set (2890 measurements). In the present study we give a dimensional justification of these variables (section 3.3). The new dimensionless variables v^{**} and q^{**} have an advantage over v^* and q^* because they account for both at-a-site and between-site variations of flow resistance and thus better describe our data.

[37] Converting our velocity and discharge measurements to the dimensionless variables v^{**} and q^{**} significantly decreased the flow resistance variation between our sites, confirming the similarity collapse achieved by *Rickenmann and Recking* [2011] for their set of flow measurements. Plots of v^{**} against q^{**} showed some scatter within each of our study reaches, but generally the data followed the same power trend with an exponent of approximately 0.6 (Figure 6). Only for very shallow flows ($q^{**} < 0.1$ or $q < 0.01$) could the trend of the data also be described by a somewhat larger exponent. There is no discontinuity in flow resistance with increasing discharge, however. In contrast to observations by *Comiti et al.* [2009] in a flume or by *David et al.* [2010] in the field this suggests a smooth transition between processes of energy dissipation, e.g., from tumbling flow to skimming flow. One reason for the smooth transition could be the less pronounced step-pool structure in our streams. Also in natural streams different locations feature different individual flow transitions at the same time, which should reduce the importance of a single transition when considering flow resistance at the reach scale.

[38] The grain size D_{84} was used by *Rickenmann and Recking* [2011] as a sole roughness length in the nondimensional variables (as used in equation (3)). We introduced alternative roughness lengths, namely boulder protrusion P, the standard deviation of profile elevations s, and step height H_s. Of these four candidates for the roughness length scale (R) in the nondimensionalization, D_{84} was superior (in terms of RMSE) in explaining the variations among the different sites. This might be due to the interdependency of channel slope S and channel roughness R. While P, s, and H_s are strongly correlated with S, the least slope-dependent roughness length is D_{84} (Figure 4). Consequently D_{84} might have more additional explanatory power than the other roughness lengths, whose effects might be already explained implicitly by the slope S itself. In other studies the standard deviation of elevations s was found to be a better roughness measure

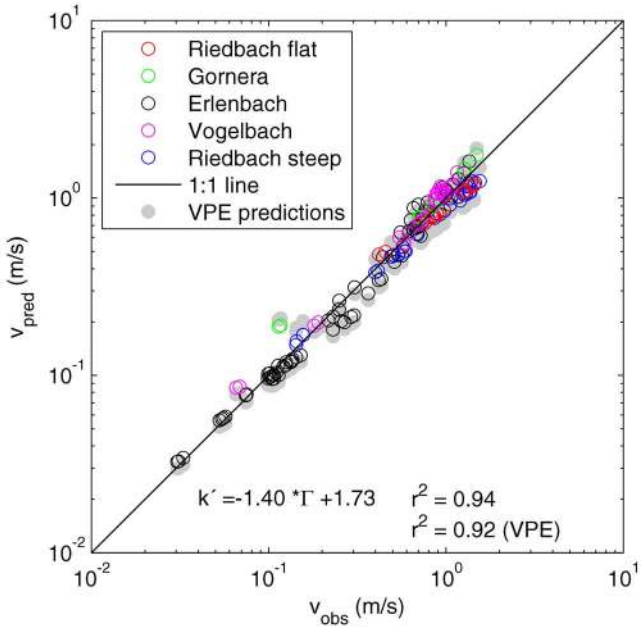

Figure 8. Predicted against observed flow velocities, where predicted velocities were calculated using equation (10). The regression equation for k' (equation (8)) was derived from the nondimensional variables v^{**} and q^{**} using $R = D_{84}$. The coefficient of determination r^2 is given for the predictions of equation (10) as well as for predictions with the variable power equation (VPE) by *Ferguson* [2007] (equation (6)).

Table 5. Scores for Flow Velocity Predictions v_{pred} Using Equation (10) (With Boulder Concentration as Dimensionless Roughness) and the Variable Power Equation (VPE) by *Ferguson* [2007] (Equation (6))[a]

	Equation (10)	VPE Equation (6)
Erlenbach	63/88	47/78
Riedbach Steep	44/93	63/85
Riedbach Flat	55/100	10/15
Gornera	40/80	0/40
Vogelbach	48/77	71/94
Mean[b]	50/88	38/62

[a]The scores are the percentage of data that were predicted within ±10%/±20% of the measured flow velocities v_{obs}.
[b]Mean value with equal weight for all stream reaches.

than D_{84} to explain variations in flow resistance [*Aberle and Smart*, 2003; *David et al.*, 2010; *Smart et al.*, 2002; *Yochum et al.*, 2012]. It is somewhat surprising that this is not the case in our study. For our study sites, the correlation between D_{84} and s is even higher if one outlier is not considered (then r^2 is 0.48, cf. Figure 4). Another factor is that in contrast to the step-pool streams in the study of *Yochum et al.* [2012] our streams have practically no steps formed by woody debris; consequently the correlation of D_{84} and s is higher.

[39] In general, channel slope shows strong correlations with several macroroughness measures (Figure 4). This means that the effects of the driving forces represented by downslope gravity channel slope and roughness cannot be separated on statistical grounds alone. But they could be distinguished physically, because they have opposite effects on flow velocity. Their scaling relationship could reflect the fact that bed roughness is generated by the inability of the flow to move sediment above some particular size, and thus that roughness and slope covary in a particular way.

[40] Since slope S and channel roughness R are contained in both dimensionless variables v^{**} and q^{**} there might be some degree of spurious correlation involved in the scaling of v^{**} and q^{**}. *Rickenmann and Recking* [2011] discussed and tested the validity of this scaling and concluded that spurious correlation is not a major problem. Furthermore, the use of v^{**} and q^{**} can be justified dimensionally (section 3.3) and the scaling exponent $m = 0.6$ in equation (7) has been shown to be theoretically correct. *Ferguson* [2007] found that several different heuristic and empirical analyses of shallow flows all converged on $(8/f_{tot})^{0.5} \propto h/D$, which is equivalent to the exponent 0.6 in a v-q or v^{**}-q^{**} plot. D is a representative grain diameter. *Ferguson* [2007] suggested this "roughness layer relation" as a default model for shallow flows without having to justify any particular interpretation of the dominant physical processes.

4.2. Between-Site Variation After Nondimensionalization

[41] Collapsing our data using the nondimensional variables v^{**} and q^{**} leaves some degree of variation between the study reaches (Figure 6). The remaining variation can be quantified by comparing the stream-specific prefactors k of the fitted power trend lines as used in equation (7). In the present study, these prefactors varied within a factor of 2 (Figure 7), and the data plot well within the range of the large data set studied by *Rickenmann and Recking* [2011] (Figure 9). However, a factor-of-6 range in the prefactors k was observed by *Rickenmann and Recking* [2011] for different sites when they included the step-pool and cascade stream data of *David et al.* [2010].

[42] The comparatively small k values of the *David et al.* [2010] data might be due to additional roughness sources that were absent in our data. The small prefactors could be influenced by the large amounts of woody debris present in many reaches studied by *David et al.* [2010], and the wood load actually has shown to significantly increase flow resistance. Furthermore, woody debris has contributed to the formation of steps and has caused complex log jams, which also added to total roughness. The co-occurrence of wood and steps is not surprising: woody debris is known to be important for the development of steps [e.g., *Church and Zimmermann*, 2007; *Hassan et al.*, 2005; *Wilcox et al.*, 2006]. Moreover, significant morphologic changes in the streams described by *David et al.* [2010] are not expected, because the runoff is snowmelt dominated and the availability of sediment is limited. The smaller grains are carried out of the reaches but the snowmelt events are hardly competent to break up larger morphologic structures, gradually resulting in a rougher bed. In our study reaches, channel-spanning steps and pools are relatively infrequent and woody debris is unimportant as a source of roughness (see Figure 1).

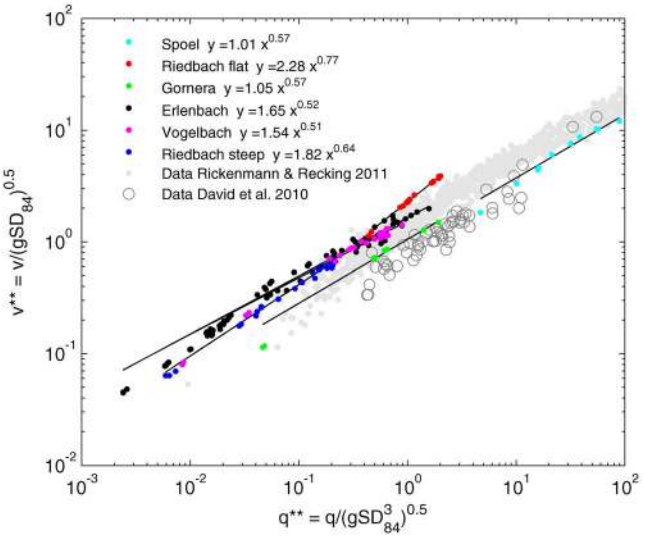

Figure 9. Dimensionless velocity v^{**} against dimensionless discharge q^{**} for at-a-site data of the present study, data of *David et al.* [2010], and the large data set of *Rickenmann and Recking* [2011], which defines a general trend of flow resistance. The lines are the fitted power trends to the data of the present study.

[43] For five reaches of the present study, the prefactors k were related to dimensionless roughness measures, i.e., boulder concentration Γ, step slope H_s/L_s, and step density n/L_r (Figure 7). Boulder concentration was best related to k, regardless of the roughness length (R) used in the nondimensionalization (Table 4). The trend line of the k-R^* relation indicates that the prefactor k increases with decreasing dimensionless roughness R^*. The trend equation (8) was used for a simple flow velocity prediction equation (equation (9)). This procedure resulted in an improvement of the flow velocity predictions compared to predictions using the VPE equation by *Ferguson* [2007] (Figure 8). The r^2 values for the agreement of predicted and observed flow velocities are somewhat better for equation (10) than for the VPE equation. Moreover, the scores for equation (10) are significantly better than for the VPE (Table 5). However, the statistical significance of the predictive regression equation should not be overrated, because there is pseudo replication with respect to boulder concentration Γ: only five independent values of Γ were used. The limited additional explanation of the residual variance explained by including Γ may be due to the fact that Γ is highly correlated with D_{84}.

[44] Only few data from natural streams are published that include both flow velocity measurements and measurements of macroroughness like boulder concentration or longitudinal

profile roughness. Thus, it is currently not possible to validate and compare the trends observed between the prefactor k and roughness measures with a larger or independent set of data. However, for some published flow resistance data, information about channel type is available. *Montgomery and Buffington* [1997] classified channel types partly according to grain sizes and dominant roughness sources, implying that channel type reflects processes and magnitudes of roughness and can be regarded as a qualitative measure of macroroughness. Based on this assumption we compared our flow velocity data (six sites) with some of the available data in the literature (*David et al.* [2010], 15 sites; *Ryan et al.* [2002], five sites; *Reid and Hickin* [2008], two sites; *Lepp et al.* [1993], two sites; *Andrews* [1994], one site). Plane bed and pool-riffle channels plot rather in the upper part of the entire data range and step-pool and cascade streams rather in the lower part (Figure 10a). Plane bed streams on average have larger k values than cascade or step-pool streams (Figure 10b). Assuming that step-pool and cascade streams represent rougher channels than plane bed and pool riffle streams, this finding confirms our previous results that the prefactor k scales with roughness. Additionally, the sorting of the k values after channel type coincides with a slope dependence of the channel type (Figure 10c). This also confirms the interdependence of macroroughness and channel slope in our data.

[45] The k value is relatively similar for step-pool and cascade streams. The median k value of the cascade streams (0.85) is only marginally smaller than the median value for step-pool reaches (0.86) (Figure 10b). But if one extreme data point was excluded from the cascade streams, the two data distributions would differ more markedly (Figure 10c). However, cascade and step-pool stream types as defined by *Montgomery and Buffington* [1997] are not straightforward to distinguish morphologically in the field. The different types of roughness elements (individual large grains or steps) often coexist in natural streams, and it is difficult to determine which one is the dominant roughness source. Therefore similar energy dissipating processes such as tumbling, jet, and wake flow over and around grains might dominate in both channel types. In the step-pool streams of our study, large immobile boulders between the steps occur frequently and might significantly contribute to total flow resistance. We currently lack a hydraulically relevant channel type classification that explicitly refers to these residual boulders as the dominant source of roughness, including channels where the boulder concentration is lower than in a typical cascade channel. Although *Bathurst* [1985] and *Ferguson* [2007] used the term boulder-bed channel, it has not been widely used in the literature.

4.3. Similarities Between a Theoretical Flow Velocity Equation and Empirical Findings

[46] Energy can be dissipated in many ways in steep streams. The dominant processes of energy dissipation depend on the flow magnitude (plunging jets or skimming flow). The magnitude of flow resistance, however, may also depend on the dominant type of macroroughness element. Thus it is possible that an individual roughness measure, e.g., step slope or boulder concentration, represents only a specific range of dissipation processes. This could explain why a single roughness measure is not sufficient to explain the between-site flow velocity variations.

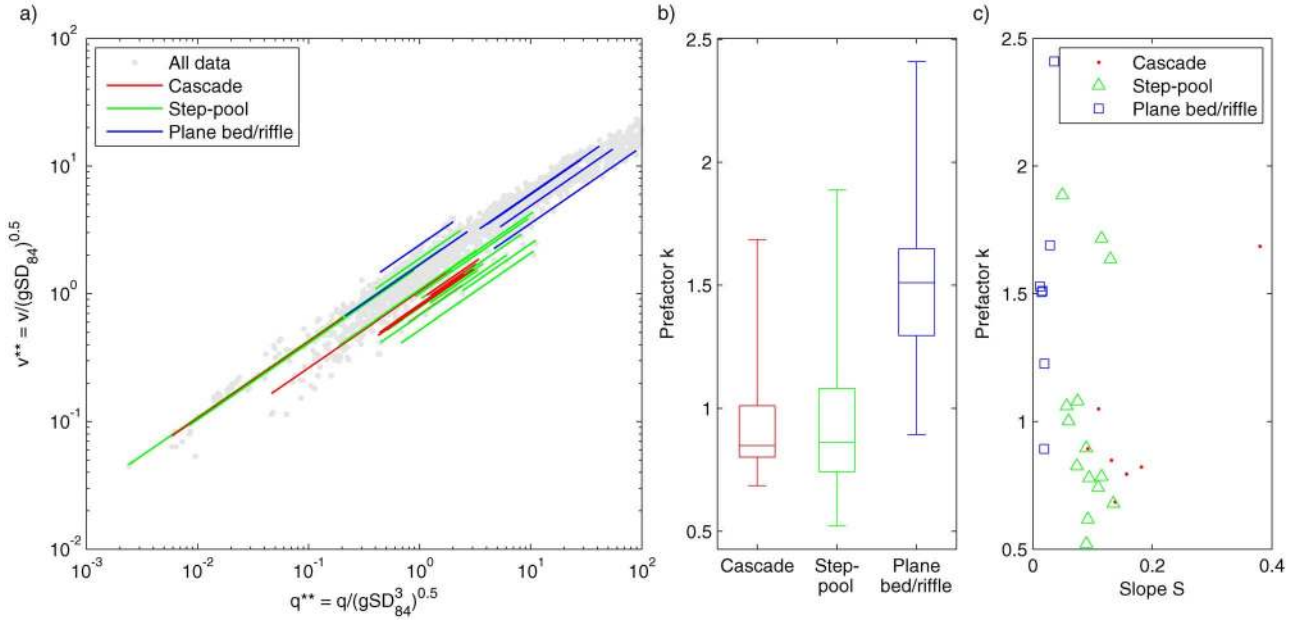

Figure 10. Relationship between channel type and at-a-site data trends. The dimensionless velocity v^{**} against dimensionless discharge q^{**} and the trend lines of the form $v^{**} = kq^{**0.6}$ (equation (7)) are given with lines colored according to channel type (Figure 10a). The derived prefactors k are plotted against channel type (Figure 10b) and channel slope (Figure 10c). Classified data sets include measurements of the present study and of *Andrews* [1994], *David et al.* [2010], *Lepp et al.* [1993], *Reid and Hickin* [2008], and *Ryan et al.* [2002]. The points in (Figure 10a) indicated as "All data" are the original data points and unclassified data used by *Rickenmann and Recking* [2011].

[47] However, our empirical analysis shows that boulder concentration, compared to other measures of macroroughness, is capable of explaining the differences in flow velocity between sites to some extent. The success of boulder concentration might be partly due to the dominance of boulders in our study channels, even in the two step-pool reaches. But the empirically observed effects are also reflected by a theoretical flow velocity equation accounting for the influence of boulders and steps. Here we discuss a flow velocity equation, the theoretical model developed by *Yager* [2006] and *Yager et al.* [2012] and test it against the measured flow velocities.

[48] *Yager* [2006] studied the influence of immobile boulders on the stresses acting on mobile grains in steep streams. Her flow equation is based on stress-partitioning between immobile and mobile grains. Boulder concentration and the boulder protrusion P emerge as the main controls on shear stresses and flow velocities, whereas boulder concentration was given by the downstream length of immobile grain-steps λ_w divided by the grain-step spacing λ_x. For resistance of the mobile sediment she assumes a constant friction coefficient $C_m = 0.44$, calculated from independent data by *Marcus et al.* [1992]. Flow resistance of the immobile material is parameterized as a friction coefficient C_I that depends on protrusion and flow depth, which are scaled with the cross-sectional area of the immobile grains A_{IF}. Rewriting the stress equations by *Yager* [2006] as the reach-averaged flow velocity gives

$$v_Y = \sqrt{\frac{2}{A_{IF}C_I/(\lambda_x w) + C_m(1-\lambda_w/\lambda_x)}}\sqrt{ghS}. \qquad (11)$$

[49] Using equation (11) predicted flow velocities were 5%–50% lower than our measurements (Figure 11a). Notably, the accuracy of the predictions generally increased with boulder concentration. The Spöl data plot a bit off the trend of the other streams, which might be due to the relatively high observed flows and large relative flow depths h/D_{84}, leading to higher flow velocities (Figure 11a). For the Gornera and Riedbach steep sites, which feature boulder concentrations larger than 12%, the predicted velocities are very close to the measurements (with deviations <5%). According to Figure 11a the influence of boulder roughness becomes important at boulder concentrations somewhere between 12% and 30%. This illustrates the importance of boulder effects on total flow resistance for higher boulder concentrations, which is a theoretical support of our empirical analysis. This is also apparent in the low ratio of base level resistance f_0 to total resistance f_{tot} at high boulder concentrations (Figure 11b). The approach of *Yager* [2006] also performed better at higher boulder concentrations in predicting bed load volumes in combination with accounting for large scale roughness [*Nitsche et al.*, 2011], which is an indirect confirmation of our findings.

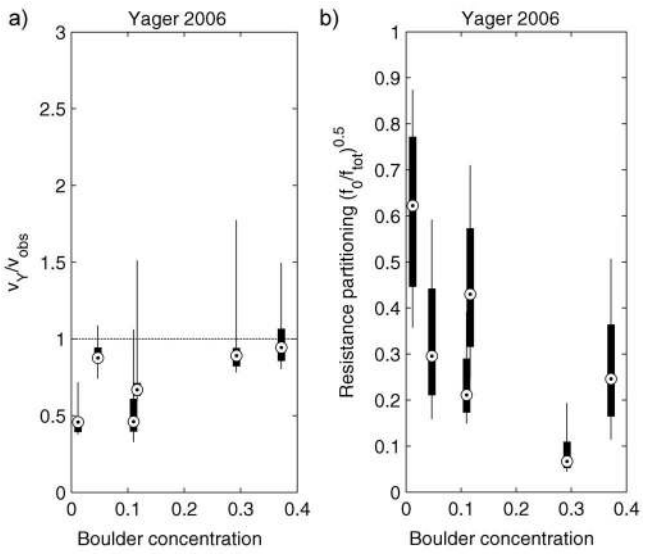

Figure 11. Calculated divided by (a) observed flow velocities and (b) base level to total flow resistance $(f_0/f_{tot})^{0.5}$ plotted against boulder concentration using the equations by *Yager* [2006] (equation (11)). Plotted are data of the six study reaches, each represented by a distinct boulder concentration. Boxes define the 25th and 75th percentile of the data, whiskers define the 5th and 95th percentile, and circles define the median values.

5. Conclusions

[50] Both channel slope and macroroughness are important factors explaining the variation of flow resistance between different sites. We found empirical and dimensional justification for the dimensionless velocity and discharge variables previously introduced by *Rickenmann and Recking* [2011]. These variables include the channel slope and a roughness length for nondimensionalization. Applying these dimensionless variables resulted in a similarity collapse around a simple power law relationship, in which the dimensionless velocity was approximately proportional to the 0.6 power of dimensionless discharge. As roughness length we used various measures of macroroughness, i.e., a characteristic grain size, the standard deviation of long profile elevations, the step height, and the boulder protrusion, all of which explained most of the observed between-site differences in flow resistance. Although channel slope and roughness have distinct physical effects on the flow, both have been shown to covary in a particular way. Channel slope, for example, correlates strongly with the standard deviation of thalweg elevations and with boulder protrusion, and thus could be used as proxy variable.

[51] The nondimensionalization suggested by *Rickenmann and Recking* [2011] did not perfectly collapse our data. To explain the remaining variation between the sites we introduced dimensionless macroroughness measures which describe the concentration of roughness elements in a channel. Among these, boulder concentration correlated best with the remaining between-site variation of flow resistance. Moreover, including boulder concentration in a simple regression-based prediction equation resulted in flow velocity predictions that were more precise than predictions with the variable power law equation (VPE), which was proposed by *Ferguson* [2007] and used by *Rickenmann and Recking* [2011]. With our approach 88% of the flow velocity data were predicted with a precision of ±20%, the VPE achieved

62%. Unlike the VPE and other flow velocity equations, the approach needs additional field measurements of boulder concentration, which can be carried out within a day for one reach. However, our regression-based equation is based on only five reaches and more data are needed to confirm its validity for predictive purposes. Another uncertainty may be due to the variability of macroroughness in time, an issue which has not been treated in the present study, but which might be important to account for in future investigations.

[52] There is some support of our empirical findings by applying the theoretically based flow resistance equation by *Yager* [2006]. This equation, which directly includes boulder concentration, performs better for our study streams with high concentrations of macroroughness elements than for those with low boulder concentrations. This is also an indication that boulder concentration is a useful measure of macroroughness for the studied mountain streams.

[53] **Acknowledgments.** We thank Alexander Beer, Fabian Blaser, Nicole Federspiel, Bruno Fritschi, Angela Klaiber, James Leuzinger, Käthi Liechti, Michael Pauli, Johannes Schneider, and Heidi Schott for helping in the field. This study was supported by the Swiss Federal Office for the Environment (contract no. 06.0083.PJ/G063-0651) and the CCES-APUNCH project of the Competence Center Environment and Sustainability within the domain of the Swiss Federal Institutes of Technology. We thank the AE, Gabrielle David, Rob Ferguson, and Francesco Comiti for detailed comments, which helped in improving this paper.

References

Aberle, J., and G. M. Smart (2003), The influence of roughness structure on flow resistance on steep slopes, *J. Hydraul. Res.*, *41*(3), 259–269.

Andrews, E. D. (1994), Marginal bed-load transport in a gravel-bed stream, Sagehen Creek, California, *Water Resour. Res.*, *30*(7), 2241–2250.

Bathurst, J. C. (1985), Flow resistance estimation in mountain rivers, *J. Hydraul. Eng.*, *111*(4), 625–643.

Bezinge, A. (1999), *Val de Zermatt GD—Prise d'eau du glacier du Gorner, tech. rep.*, Grande Dixence SA, Sion, Switzerland.

Bray, D. I. (1979), Estimating average velocity in gravel-bed rivers, *J. Hydraul. Div.*, *105*(9), 1103–1122.

Canovaro, F., and L. Solari (2007), Dissipative analogies between a schematic macroroughness arrangement and step-pool morphology, *Earth Surf. Processes Landforms*, *32*, 1628–1640.

Chin, A. (2003), The geomorphic significance of step-pools in mountain streams, *Geomorphology*, *55*, 125–137.

Chin, A., and E. Wohl (2005), Toward a theory for step pools in stream channels, *Progress Phys. Geogr.*, *29*(3), 275–296, doi:10.1191/0309133305 pp449ra.

Church, M., and A. Zimmermann (2007), Form and stability of step-pool channels: Research progress, *Water Resour. Res.*, *43*(3), W03415, doi:10.1029/2006WR005037.

Comiti, F., L. Mao, A. Wilcox, E. E. Wohl, and M. A. Lenzi (2007), Field-derived relationships for flow velocity and resistance in high-gradient streams, *J. Hydrol.*, *340*, 48–62, doi:10.1016/j.jhydrol.2007.03.021.

Comiti, F., D. Cadol, and E. Wohl (2009), Flow regimes, bed morphology, and flow resistance in self-formed step-pool channels, *Water Resour. Res.*, *45*(4), W04424, doi:10.1029/2008WR007259.

David, G. C. L., E. Wohl, S. E. Yochum, and B. P. Bledsoe (2010), Controls on spatial variations in flow resistance along steep mountain streams, *Water Resour. Res.*, *46*(3), W03513, doi:10.1029/2009WR008134.

Egashira, S., and K. Ashida (1991), Flow resistance and sediment transportation in streams with step-pool bed morphology, in *Fluvial Hydraulics of Mountain Regions*, pp. 45–58, Springer, Heidelberg.

Farinotti, D., M. Huss, A. Bauder, and M. Funk (2009), An estimate of the glacier ice volume in the Swiss Alps, *Global Planet. Change*, *68*, 225–231, doi:10.1016/j.gloplacha.2009.05.004.

Fehr, R. (1987), Einfache bestimmung der korngrössenverteilung von geschiebematerial, *Schweizer Ingenieur Architekt*, *105*(38), 1004–1109.

Ferguson, R. (2007), Flow resistance equations for gravel- and boulder-bed streams, *Water Resour. Res.*, *43*(12), W05427, doi:10.1029/2006WR005422.

Foster, I. D. L., Ed. (2000), *Tracers in Geomorphology*, Wiley, Chichester.

GSF (1978), *Jahresbericht, Institut für Hydrologie des Forschungszentrum für Umwelt und Gesundheit gsf*, Gesellschaft für Strahlenforschung, Neuherberg.

Hassan, M. A., M. Church, T. E. Lisle, F. Brardinoni, L. Benda, and G. E. Grant (2005), Sediment transport and channel morphology of small, forested streams, *J. Am. Water Resour. Assoc.*, *04072*, 853–876.

Hey, R. D. (1979), Flow resistance in gravel-bed rivers, *J. Hydraul. Div.*, *105*(4), 365–379.

Kilpatrick, F. A., and J. F. J. Wilson (1989), *Measurement of time of travel and dispersion in streams by dye tracing*, U. S. Geological Survey, Water Resources Division, Reston, VA.

Lamarre, H., and A. G. Roy (2008), A field experiment on the development of sedimentary structures in a gravel-bed river, *Earth Surf. Processes Landforms*, *33*, 1064–1081.

Lee, A. J., and R. I. Ferguson (2002), Velocity and flow resistance in step-pool streams, *Geomorphology*, *46*, 59–71.

Leibundgut, C., P. Maloszewski, and C. Külls (2009), *Tracers in Hydrology*, 415 pp., Wiley-Blackwell, London.

Lepp, L. R., C. J. Koger, and J. A. Wheeler (1993), Channel erosion in steep gradient, gravel-paved streams, *Bull. Assoc. Eng. Geol.*, *30*(4), pp. 443–454.

MacFarlane, W. A., and E. Wohl (2003), Influence of step composition on step geometry and flow resistance in step-pool streams of the Washington Cascades, *Water Resour. Res.*, *39*(2), 1037, doi:10.1029/2001WR001238.

Marcus, W. A., K. Roberts, L. Harvey, and G. Tackman (1992), An evaluation of methods for estimating Manning's *n* in small mountain streams, *Mountain Res. Dev.*, *12*(3), 227–239.

Montgomery, D. R., and J. M. Buffington (1997), Channel-reach morphology in mountain drainage basins, *Geol. Soc. Am. Bull.*, *109*(5), 596–611.

Nelson, P. A., J. G. Venditti, W. E. Dietrich, J. W. Kirchner, H. Ikeda, F. Iseya, and L. S. Sklar (2009), Response of bed surface patchiness to reductions in sediment supply, *J. Geophys. Res.-Earth Surf.*, *114*, F02005.

Nitsche, M., D. Rickenmann, J. M. Turowski, A. Badoux, and J. W. Kirchner (2011), Evaluation of bedload transport predictions using flow resistance equations to account for macro-roughness in steep mountain streams, *Water Resour. Res.*, *47*(8), W08513, doi:10.1029/2011WR010645.

Pagliara, S., and P. Chiavaccini (2006), Flow resistance of rock chutes with protruding boulders, *J. Hydraul. Eng.*, *132*(6), 545–552.

Reid, D. E., and E. J. Hickin (2008), Flow resistance in steep mountain streams, *Earth Surf. Processes Landforms*, *2008*(33), 2211–2240, doi:10.1002/esp.1682.

Rickenmann, D. (1994), An alternative equation for the mean velocity in gravel-bed rivers and mountain torrents, paper presented at Hydraulic Engineering '94, American Society of Civil Engineers, Buffalo, NY.

Rickenmann, D. (1996), Fliessgeschwindigkeit in wildbächen und gebirgsflüssen, *Wasser Energie Luft*, *88*(11/12), 298–304.

Rickenmann, D., and A. Recking (2011), Evaluation of flow resistance in gravel-bed rivers through a large field data set, *Water Resour. Res.*, *47*(7), W07538, doi:10.1029/2010WR009793.

Ryan, S. E., L. S. Porth, and C. A. Troendle (2002), Defining phases of bedload transport using piecewise regression, *Earth Surf. Processes Landforms*, *27*(9), 971–990, doi:10.1002/Esp.387.

Schnegg, P.-A. (2003), A new field fluorometer for multi-tracer tests and turbidity measurement applied to hydrogeological problems, in *8th International Congress of the Brazilian Geophysical Society*, Brazilian Geophysical Society, Rio de Janeiro, Brazil.

Schnegg, P.-A., and N. Doerflinger (1997), An inexpensive flow-through field fluorometer, in *6th Conference on Limestone Hydrology and Fissured Media*, 4 pp., la Chaux-de-Fonds, Univ. of Franche-Comté, Besançon, France, [Available online at http://www-geol.unine.ch/GEOMAGNETISME/uis97.pdf].

Smart, G. M., M. J. Duncan, and J. M. Walsh (2002), Relatively rough flow resistance equations, *J. Hydraul. Eng.*, *128*(6), 568–578.

Smart, G., J. Aberle, M. Duncan, and J. Walsh (2004), Measurement and analysis of alluvial bed roughness, *J. Hydraul. Res.*, *42*(3), 227–237.

Thompson, S. M., and P. L. Campbell (1979), *Hydraulics of a Large Channel Paved With Boulders*, pp. 341–354, Taylor & Francis, London.

Turowski, J. M., E. M. Yager, A. Badoux, D. Rickenmann, and P. Molnar (2009), The impact of exceptional events on erosion, bedload transport and channel stability in a step-pool channel, *Earth Surf. Processes Landforms*, *34*, 1661–1673.

Waldon, M. G. (2004), Estimation of average stream velocity, *J. Hydraul. Eng.*, *130*(11), 1119–1122.

Weingartner, R., and H. Aschwanden (1992a), Discharge regime—The basis for estimation of average flows, in *Hydrological Atlas of Switzerland*, p. Plate 5.2, Swiss Federal Office for the Environment, Bern.

Weingartner, R., and H. Aschwanden (1992b), Mean annual corrected precipitation depths 1951–1980, in *Hydrological Atlas of Switzerland*, p. Plate 2.2, Swiss Federal Office for the Environment, Bern.

Whittaker, J. G. (1986), An equation for predicting bedload transport in steep mountain step-pool stream, in *9th Australasian Fluid Mechanics Conference*, Univ. of Auckland, Auckland, New Zealand.

Whittaker, J. G., and M. N. R. Jaeggi (1982), Origin of step-pool systems in mountain streams, *J. Hydraul. Div.*, *108*(6), 758–773.

Whittaker, J. G., W. E. Hickman, and R. N. Croad (1988), *Riverbed stabilisation with placed blocks*, Central Laboratories, Works and Development Corporation, Lower Hutt, NZ.

Wilcox, A. C., J. M. Nelson, and E. E. Wohl (2006), Flow resistance dynamics in step-pool channels: 2. Partitioning between grain, spill, and woody debris resistance, *Water Resour. Res.*, *42*, W05419, doi:10.1029/2005WR004278.

Yager, E. M. (2006), Prediction of sediment transport in steep, rough streams, Ph.D. thesis, 232 pp, University of California, Berkeley, Berkeley.

Yager, E. M., J. W. Kirchner, and W. E. Dietrich (2007), Calculating bed load transport in steep boulder bed channels, *Water Resour. Res.*, *43*, W07418, doi:10.1029/2006WR005432.

Yager, E. M., W. E. Dietrich, J. W. Kirchner, and B. W. McArdell (2012), Prediction of sediment transport in step-pool channels, *Water Resour. Res.*, *48*(1), W01541, doi:10.1029/2011WR010829.

Yochum, S. E., B. P. Bledsoe, G. C. L. David, and E. Wohl (2012), Velocity prediction in high-gradient channels, *J. Hydrol.*, *424–425*, 84–98, doi:10.1016/j.jhydrol.2011.12.031.

Zimmermann, A. (2010), Flow resistance in steep streams: An experimental study, *Water Resour. Res.*, *46*, W09536, doi:10.1029/2009WR007913.

Zimmermann, A. E., M. Church, and M. A. Hassan (2008), Identification of steps and pools from stream longitudinal profile data, *Geomorphology*, *102*, 395–406.